Phonon Energies in Germanium from Phonon-Assisted Tunneling*†

R. T. PAYNE‡§
Department of Physics and Institute for the Study of Metals, University of Chicago, Chicago, Illinois
(Received 18 February 1965)

The line shapes of the peaks in the bias dependence of the second derivative of the phonon-assisted tunnel current with respect to voltage were measured for Sb-doped germanium tunnel junctions between 4.2 and 1.15°K. The antimony concentration was 5×10^{18} cm^{-3}. The phonon energies at the point L in the Brillouin zone, determined to an accuracy of $\pm0.1\%$, are $E(\mathrm{TA})=7.766$, $E(\mathrm{LA})=27.58$, $E(\mathrm{LO})=30.62$, and $E(\mathrm{TO})=36.15$ in meV. This accuracy verifies the assumptions made in determining the pressure dependence of these phonon energies previously reported by the author. The major contribution to the line shapes is kT broadening. Minor contributions arise from a small bias dependence of the tunnel current per energy interval and from the phonon dispersion near L. Approximate values for the curvatures of the phonon spectrum at L were determined. A lower limit of 1.6×10^{-11} sec was found for the lifetimes of these phonons. From double phonon emission processes the energy of the optic phonon at Γ was found to be 37.3 ± 0.2 meV.

I. INTRODUCTION

THE presence of phonon-assisted electronic tunneling in narrow p-n junctions of semiconductors provides a powerful tool for measuring some properties of semiconductor lattice vibrations.[1–4] At temperatures below 4.2°K where only spontaneous phonon emission need be considered, the current-versus-bias-voltage (I-V) curve of a typical junction shows a sharp change in slope at the onset voltage for emission of certain phonons.[3] The onset voltage equals the energy of phonons with wave number equal to the crystal momentum difference between the conduction and valence band extrema of the semiconductor.[4–6] Because the second derivative of a sharp change in slope appears as a large peak, the measurement of the second derivative in current with respect to voltage as a function of bias voltage (d^2I/dV^2-V) appears to be the best method for determining the phonon energy.[6,7]

It is the purpose of this paper to describe the measurement of (d^2I/dV^2-V) for p-n junctions of germanium doped to 5×10^{18} atoms/cm^3 with antimony to obtain the phonon energies at the symmetry point L, the (111) intersection with the Brillouin zone boundary of germanium. A high degree of accuracy was needed to verify the stress dependence of the phonon energies previously reported.[8]

The line shape of the second-derivative peak can largely be explained in terms of the second derivative with respect to voltage of the Fermi distribution functions found in the expression for the tunneling current. Analysis of the experimental data brings to light two effects contributing to the line shape of second-derivative peaks not previously considered: a step-function distortion to the line shape, and low-temperature broadening of the line shape. The first effect can be explained in terms of the voltage dependence of electron tunneling probability.[1,2] The second effect can be understood in terms of phonon dispersion around the symmetry point. This effect leads to an estimate of the curvature of the phonon spectrum around the symmetry point. Certain peaks in (d^2I/dV^2-V) are attributed to double-phonon–assisted electronic tunneling. This provides a means of measuring the phonon energy of the optic branch at the point Γ, the Brillouin zone (BZ) center.

This paper consists of four parts: a general consideration of the problem, a discussion of the experimental arrangement, the analysis of data resulting from the experiment, and a summary of the results.

II. GENERAL CONSIDERATIONS

In order to study the phonon properties found in phonon-induced electronic tunneling, one must first consider the electronic or Esaki-type tunneling process[9] for semiconductors itself. Electronic tunneling can be observed when the depletion region between a p-type and an n-type material of the same host or base semiconductor is sufficiently narrow, less than 300 Å.[9,10] It is further required that the p-type and n-type materials of the host semiconductor be sufficiently doped to have a

* Submitted as a thesis in partial fulfillment of the requirements for the degree of Doctor of Philosophy at The University of Chicago.

† Supported in part by the U. S. Air Force Office of Scientific Research through Grant No. AF-AFOSR 148-63.

‡ An Advanced Research Projects Agency Research assistant.

§ Present address: Department of Physics, University of Pennsylvania, Philadephia, Pennsylvania.

[1] L. V. Keldysch, Zh. Eksperim. i Teor. Fiz. **34**, 962 (1958) [English transl.: Soviet Phys.—JETP **7**, 665 (1958)].

[2] E. O. Kane, J. Appl. Phys. **32**, 83 (1961).

[3] N. Holonyak *et al.*, Phys. Rev. Letters **3**, 167 (1959).

[4] R. N. Hall, *Proceedings of the International Conference on Semiconductors, Prague, 1960* (Czechoslovak Academy of Sciences, Prague, 1961), p. 193.

[5] B. N. Brockhouse and P. K. Iyengar, Phys. Rev. **111**, 747 (1958).

[6] A. G. Chynoweth, R. A. Logan, and D. E. Thomas, Phys. Rev. **125**, 877 (1962).

[7] R. A. Logan, J. M. Rowell, and F. A. Trumbore, Phys. Rev. **136**, A1751 (1964).

[8] R. T. Payne, Phys. Rev. Letters **13**, 53 (1964).

[9] L. Esaki, Phys. Rev. **109**, 603 (1958).

[10] E. O. Kane, J. Phys. Chem. Solids **12**, 181 (1959).

well-defined Fermi surface in the valence and conduction bands, respectively, at absolute zero temperature.[9,11]

With the help of simple theoretical arguments, the character of the phonon-assisted electronic tunneling process can be obtained.[1,2,12] The phonon-assisted tunneling current I can be written for a narrow semiconductor p-n junction at a low temperature T, where only spontaneous phonon emission need be considered as

$$I=\sum_{E_b(\mathbf{q})}\int f(E)\{1-f[E+eV-E_b(\mathbf{q})]\}G\,dE, \quad (1)$$

where $f(E)$ is the Fermi distribution function for an electron of energy E, V is the bias voltage across the junction, and $E_b(\mathbf{q})$ is the energy of a phonon with wave number $\mathbf{q}$ on the branch b of the reduced Brillouin zone (BZ). The function $G\,dE$ is the current contribution from an energy interval dE around the initially occupied state E to a final unoccupied state $E+eV-E_b(\mathbf{q})$ at constant voltage V and given phonon energy $E_b(\mathbf{q})$.

By convention, positive current I has been defined for tunneling from the n-type material to the p-type material. It gives its major contribution for forward bias, $V>0$. The reverse tunneling current from the p-type material to the n-type material is formed by interchanging the Fermi functions and changing the sign of $E_b(\mathbf{q})$. Figure 1 shows an example of the I-V curve of a Sb-doped germanium tunnel diode at 4.2°K.

If the sum over $E_b(\mathbf{q})$ is ignored, one can see that Eq. (1) predicts for I a sharp change in slope at the onset voltage $V_t=E_b(\mathbf{q})/e$ for $T=0$. Because of the kT broadening of the Fermi functions at finite temperatures, the change in slope takes place within a voltage range of about kT/e.

So far, the presence of the sum over all phonon energies would serve to destroy any distinct onset

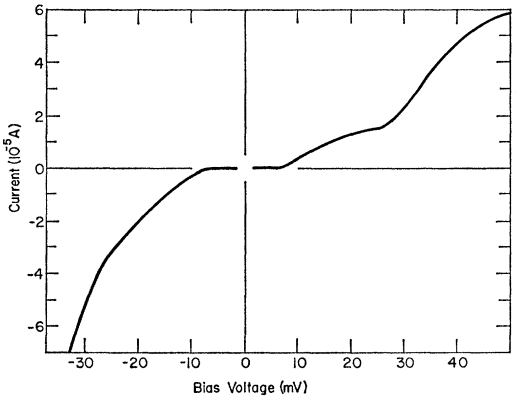

FIG. 1. Current versus bias-voltage characteristic for a phonon-assisted tunnel junction at 4.2°K. Two phonon-emission thresholds, the TA and LA branches, are observable for the antimony-doped germanium junction, D1B.

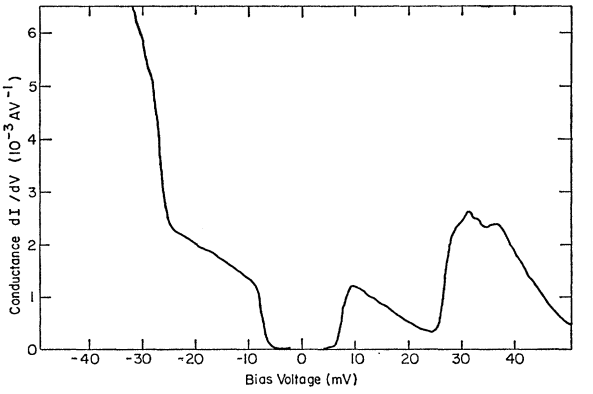

FIG. 2. First derivative in current with respect to voltage versus bias-voltage characteristic for a phonon-assisted tunnel junction at 4.2°K. Four phonon-emission thresholds, the TA, LA, LO, and TO branches, are observable for the antimony-doped germanium junction, D1B.

voltage. Experimental evidence indicates that for all practical purposes, the wave number $\mathbf{q}$ is equal to the difference in crystal momentum of the initial and final electronic states.[5,6,13] Therefore, the sum over $\mathbf{q}$ can be kept to roughly the extension $\mathbf{K}$ of the two Fermi surfaces in the BZ.

To test this condition and to unambiguously determine the phonon energies, it is necessary to locate the position of the valence- and conduction-band extrema. This can best be done if the extrema are at BZ symmetry points.

The work of Lax and Hopfield[14] clearly indicates that for germanium, the valence-band maximum is centered at Γ, the BZ center; and the conduction-band minima are located at the L points which are the four equivalent intersections of the [111] direction with the BZ boundary. The extensions of the Fermi surfaces can be made quite small on the p- and n-type sides of the junction by decreasing the doping concentrations. Further, antimony-doped germanium base materials of doping concentration around 5×10^{18} atoms/cm^3 produce very good phonon-assisted indirect tunneling characteristics[3,4,15] because of the small central-cell potential of the antimony donors.[16] Finally, if phonons are emitted around the point L in germanium then four phonon branches will be revealed: the longitudinal (LA) and transverse (TA) acoustic, and the longitudinal (LO) and transverse (TO) optic.[5]

The first measurement of all four of the phonon-induced tunneling threshold voltages V_t was made not by recording the I-V curve but by recording the first derivative in current with respect to voltage vs voltage (dI/dV-V).[4] See Fig. 2 for an example of Sb-doped germanium. A rough agreement of the step-like phonon thresholds with indirect optical transition measurements

[11] T. Yajima and L. Esaki, J. Phys. Soc. Japan **13**, 1281 (1958).
[12] J. J. Tiemann and H. Fritzsche, Phys. Rev. **137**, A1910 (1965).
[13] R. N. Brockhouse, Phys. Rev. Letters **2**, 1256 (1959).
[14] M. Lax and J. J. Hopfield, Phys. Rev. **124**, 115 (1961).
[15] Y. Furukawa, J. Phys. Soc. Japan **15**, 1903 (1960).
[16] H. Fritzsche and J. J. Tiemann, Phys. Rev. **130**, 617 (1963).

was obtained.[17,18] The accuracy of determining $E_b(\mathbf{q})$ from such a measurement is limited by the difficulty in finding the point of maximum slope. Table I gives the measured phonon energies found by indirect optical transition measurements (rows 1 and 2), and by (dI/dV-V), (row 4).

Later Chenowyth *et al.*[6] measured $(d^2I/dV^2)(dI/dV)^{-2}$ versus bias voltage and obtained peaks corresponding to the phonon threshold $V_t=E_b(L)$. See Fig. 3 for an example of (d^2I/dV^2-V) for Sb-doped germanium. This technique promised the greatest accuracy and for germanium it showed the agreement of the peak voltages to be within the experimental limit for the phonon energies $E_b(L)$ of the point L found by neutron spectroscopy data[5] (rows 6 and 5, respectively, of Table I).

It is therefore safe to assume that for germanium the major contribution to the peak amplitude in the d^2I/dV^2 comes from the phonons $E_b(L)$ near the symmetry point L. By detailed analysis of the peak line shape as a function of temperature and stress, further information about the phonon spectrum may be obtained.

The peak in the d^2I/dV^2 can be seen by differentiating Eq. (1)

$$\frac{d^2I}{dV^2}=\sum_{E_b(\mathbf{q})}\left\{-\int f\frac{d^2f(V)}{dV^2}GdE \qquad (2a)\right.$$

$$-2\int f\frac{df(V)}{dV}\frac{dG}{dV}dE \qquad (2b)$$

$$\left.+\int f[1-f(V)]\frac{dG^2}{dV^2}dE\right\}, \qquad (2c)$$

where

$$f(V)=f[E+eV-E_b(\mathbf{q})], \quad \text{and} \quad f=f(E).$$

Most of the models so far proposed for direct and indirect tunneling[1,2,12,19–21] indicate that G, dG/dV, and d^2G/dV^2 are slowly changing functions of E and V in the region of interest around the Fermi level. It is not unreasonable, then, to assume in the following discussion that G, dG/dV, and d^2G/dV^2 are constant in the small voltage range around V_t and may be moved outside the integral. If only the term $E_b(L)$ in the sum over $E_b(\mathbf{q})$ is considered, then the term (2a) generates a peak at $eV_t=E_b(L)$. The peak is symmetric in bias $(V-V_t)$ and can be reduced to a temperature-independent curve by normalizing the peak amplitude to unity and plotting the bias in units of $e(V-V_t)/kT$. This symmetrical, normalized curve is called the simple line shape in this paper.

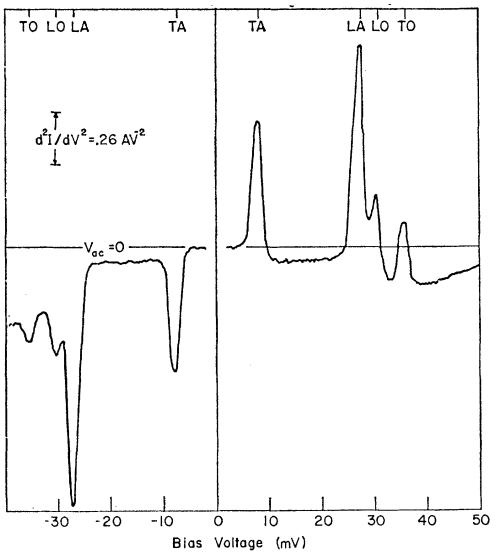

FIG. 3. Second derivative in current with respect to voltage versus bias-voltage characteristic for a phonon-assisted tunnel junction at 4.2°K. Four phonon-emission thresholds are observed and labeled for both positive and negative bias voltage. Sample is an antimony-doped germanium junction, *D1B*.

TABLE I. Summary of phonon energy determinations for the point L in the Brillouin zone of germanium.

Method	Branch TA (meV)	LA (meV)	LO (meV)	TO (meV)	Error
Absorption spectra	7.76	27.6	30.2	36.2	···
Recombination radiation	9.1	27.4	···	35.9	···
I-V	7.9	27.5	···	···	1.8%
dI/dV-V	8.0	27.7	31.3	36.3	2%
Neutron spectroscopy	8.0	26.6	30.5	34.7	±1.2 meV[a]
$d^2I/dV^2(dI/dV)^{-2}-V$	7.6	27.5	31.6	36.0	±2%
d^2I/dV^2-V	7.6	27.5	31.1	36.3	±0.2 meV
This experiment	7.766	27.58	30.62	36.15	±0.1%

[a] Except for the TA which is ±0.4 meV.

It is necessary to consider distortions from the simple line shape in order to understand the minor contributions to the second derivative which might shift the maximum away from $E_b(L)$. Two distortions will be considered in the light of the present experimental data.

First, if G varies as a function of V and the sum over $E_b(\mathbf{q})$ is again ignored, then terms (2b) and (2c) introduce step functions and changes in slope, respectively, at the threshold V_t at $T=0$. Only term (2b) will be considered at this time. Term (2c) should be an order of magnitude smaller than (2b) and is roughly constant in the region around V_t. The effect of the term

[17] G. G. Macfarlane *et al.*, J. Phys. Chem. Solids **8**, 388 (1959).
[18] J. R. Haynes, M. Lax, and W. F. Flood, J. Phys. Chem. Solids **8**, 392 (1959).
[19] P. J. Price and J. M. Radcliffe, IBM J. Res. Develop. **3**, 364 (1959).
[20] W. P. Dumpke, P. B. Miller, and R. R. Haering, J. Phys. Chem. Solids **23**, 501 (1962).
[21] R. E. Prange, Phys. Rev. **131**, 1083 (1963).

(2b) can be seen in Fig. 4(b) for a finite temperature. The superposition of terms like (2a) and (2b), shown separately in Fig. 4(a), can cause a considerable change in peak position depending on the temperature dependence of $d^2f(V)/dV^2$, and the ratio $(dG/dV)G^{-1}$ at $E_b(\mathbf{q})=eV_t$. However, the average of the absolute magnitudes of the peak voltages for positive and negative bias will tend to be equal to V_t if $(dG/dV)G^{-1}$ does not change sign and is a slowly varying function of V. This can be seen by noting that (2a) changes sign for negative bias and reverse current while (2b) does not.

The second type of distortion from the simple line shape is due to the summation over $E_b(\mathbf{q})$. The line shape will have roughly a temperature-independent part which reflects the phonon dispersion curve for a region in q around the symmetry point at absolute zero

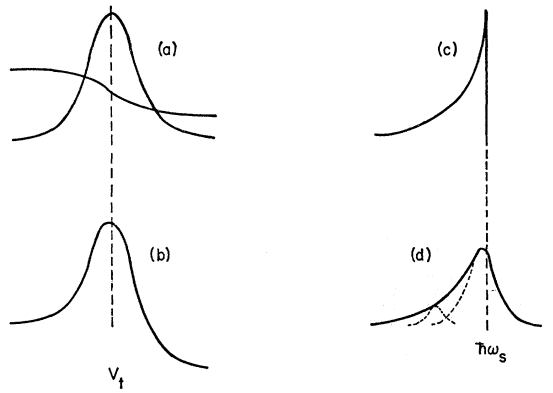

FIG. 4. Distortions to the simple line shape. Two types of distortion are present in $(d^2I/dV^2\text{-}V)$ line shapes at the threshold for phonon emission at symmetry point. First, superposition of step function and simple line shape (a) at finite temperature produces distortion (b). Second, phonon dispersion (c) at absolute zero temperature causes roughly a temperature-independent broadening of simple line shape at finite temperature (d). Both these effects shift the peak voltage from the value given by the phonon energy at the symmetry point.

temperature. For example, the dispersion curve in Fig. 4(c) causes the absolute magnitude of the positive and negative bias peak voltages to vary with temperature because of the superposition of the simple line shapes for each $E_b(\mathbf{q})$, as shown in Fig. 4(d). The uncertainty in measuring $E_b(L)$ will depend to a large extent on the type of dispersion present. By measuring the average V_p of the absolute magnitudes of the forward and reverse peak voltages as a function of T and by finding the temperature dependence of the half-width, information about the phonon dispersion curve may be obtained.

III. EXPERIMENTAL ARRANGEMENT

A. Samples, Sample Holder, and Cryostat

The samples listed in Table II were prepared by cutting rectangular bars (indexed by number in column 1) from slices (indexed by first letter in column 1) of n-type, Sb-doped germanium single crystals pulled from the melt. The rough dimensions of the bars were 1 mm $\times$1 mm$\times$14 mm after cutting and etching. They were oriented to within 1° of the crystallographic axis listed in columns 2 and 3. The carrier concentration was obtained by measuring the resistivity and Hall coefficient of a similar bar next to the sample (column 4).

TABLE II. Electronic and crystallographic properties of p-n junctions used in experiment.

Junction name	Crystallographic orientation Stress	Current	Impurity concentration (10^{18} cm^{-3})	n-type Fermi level meV	I_p (300°K) (10^{-5} A)	I_v (300°K) (10^{-5} A)
A1A	0$\bar{1}$1	110	5.07	19.6	5.4	2.95
A1B	0$\bar{1}$1	110	5.07	19.6	3.0	1.61
A2A	011	100	5.07	19.6	0.75	0.55
A2B	011	100	5.07	19.6	1.33	0.85
A3A	011	100	5.07	19.6	3.9	2.3
A3B	011	100	5.07	19.6	2.9	1.9
B1A	···	111	4.5	18.8	2.3	1.65
B1B	···	111	4.5	18.8	5.04	4.00
C1A	001	110	7.68	26.0	16.3	7.1
C1B	001	110	7.68	26.0	11.7	7.6
D1A	001	110	12.5	36.0	12.4	4.8
D1B	001	110	12.5	36.0	22.2	8.7

Tunnel junctions were prepared by placing 0.3-mm-diameter pellets of indium alloyed with 0.68% gallium on the etched germanium bars and heating to approximately 500°C for periods of a minute or less in a hydrogen atmosphere.[22] A platinum-wire loop was embedded in the indium-gallium alloy dot. Another platinum-wire loop was soldered with Cerroseal close to the junctions in order to keep the "ohmic" resistance of the germanium bar at a minimum. This soldered connection was varied from 0.3 mm to 0.9 mm away from the tunnel junctions without causing any change in the experimental results. Then the sample was etched in CP-4 until the proper peak current[23,24] I_p and the valley current[25] I_v were obtained (Table II, columns 6 and 7). This etch also served to remove junction material of different orientation and resulted in a more uniform definition of the tunneling direction.

Figure 5 is a sketch of a sample (A) with one junction each (D) on opposing faces of the bar, and the soldered connection (C) in between. The two junctions are used to compensate for possible flexure of the bar under uniaxial compression (along E in Fig. 5) and to provide two independent measurements for a given carrier concentration. The n-type Fermi level is listed in Table II, column 5. The p-type Fermi level is estimated to be 140 meV for junctions made by the process described.[16]

[22] Junctions of this type usually have regrowth regions of the order of 160μ. M. I. Nathan and S. H. Moll, IBM J. Res. Develop. 3, 375 (1962).
[23] Y. Furukawa, J. Phys. Soc. Japan **15**, 730 (1960).
[24] J. J. Tiemann and H. Fritzsche, Phys. Rev. **132**, 2506 (1963).
[25] R. S. Claassen, J. Appl. Phys. **32**, 2372 (1961).

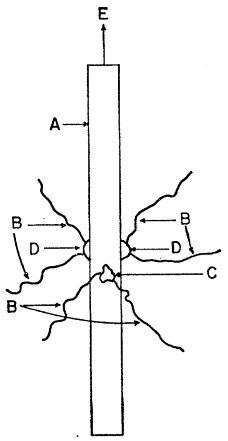

FIG. 5. *p-n* junction construction for stress experiments. A square bar of base material (A) is alloyed to make *p-n* junctions (D). Then platinum-wire loops (B) are embedded in the alloyed dot. Finally, "ohmic" connection (C) is made with low-temperature solder. This sample is then placed in a stressing rig for uniaxial compression along the line (E).

Because stress effects were also measured during the experiment, the ends of the sample bar were fastened to 0.45-cm-diam brass cups with epoxy. Nylon sleeves covered each cup to provide electrical insulation for the bar. This assembly was placed in the jaws of a uniaxial compressional stressing rig[26] which operated at helium temperatures and formed the sample holder.

In order to obtain a four-terminal potentiometric measurement, one lead (B in Fig. 5) from each connection on the sample was designated as the current lead and the other, the voltage lead. The six leads from the bar were all strung from the sample holder in the low-temperature cryostat to the measuring circuit.

Attached to the side of the sample holder was a carbon resistor thermometer which was calibrated by a helium vapor-pressure manometer to an absolute accuracy of 1%. The carbon thermometer had been heat cycled to 77°K a number of times to obtain a stability of 0.1% or better.

Finally, the sample holder was covered with a copper can to exclude light radiation and improve temperature stability. This system was then immersed in liquid helium in the cryostat.

The cryostat was a double-Dewar helium system which could be evacuated. The temperature range obtainable was from 4.2° to 1.11°K. By using a Cartesian manostat, the temperature above the lambda point could be regulated to 0.1% for periods of one hour or more.

B. Electronics

For each junction, three types of curves were needed for this experiment. The I-V curve plotted at 300°, 77°, and 4.2°K was used to make sure that these junctions were similar to those described in previous experiments.[8,16] The $(dI/dV$-$V)$ curve was used to make corrections needed to obtain the third type of curve, the $(d^2I/dV^2$-$V)$ curve.

By measuring, as a function of a slowly varying bias voltage, the dc current I_{dc}, the ac current $I(f)$, and the first-harmonic current distortion $I(2f)$ of a small fixed ac voltage, the I-V, $(dI/dV$-$V)$, and $(d^2I/dV^2$-$V)$ curves of the junction can be obtained.

Figure 6 schematizes the low-impedance circuit used to generate the dc and ac voltages needed to bias the junction and pick up the current, I_{dc}, $I(f)$, and $I(2f)$. The current was amplified, filtered, converted to a dc voltage, and plotted continuously against the voltage drop V across the tunnel junctions by an X-Y recorder (see Fig. 7). Sweep rates were kept sufficiently low to introduce no more than 2% error in the current axis.

The dc bias voltage V_{dc} was generated across a 1.15-Ω ten-turn single-wire potentiometer R_{dc} by a Willard cell C with a current-limiting resistance R_L (Fig. 6). I_{dc}, $I(f)$, and $I(2f)$ were measured for each junction as a function of bias V by motor driving the potentiometer R_{dc}.

The ac voltage V_{ac} was generated from a filtered audio generator V_g and stepped down to a voltage of 0–300 μV by the transformer T_g (Fig. 6). The transformer had a voltage ratio of 1000 to 1 and a low impedance winding resistance of less than 1 Ω. The audio generator was stable to better than 1% per day.

I_{dc} was detected by substituting a 100-Ω resistance R_d for the detecting transformer T_d shown in Fig. 6. The voltage drop across R_d was applied to the V axis of an X-Y recorder (Fig. 7).

$I(f)$ and $I(2f)$ were measured by using T_d (Fig. 6), which is identical in construction to T_g, as a current to voltage converter. The equivalent resistance of this converter was roughly 4.4×10^3 Ω at 100 cps.

A rejection filter for the first harmonic was introduced between the audio-signal generator (Fig. 7) and the low-impedance circuit to reduce the distortion of V_g to a minimum. When measuring $I(2f)$, the output V_0(ac)

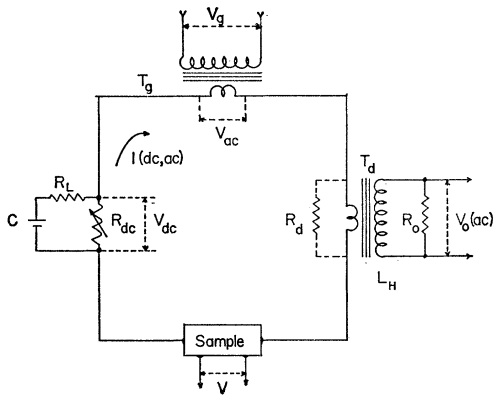

FIG. 6. Schematic drawing of low-impedance circuit used in this experiment.

[26] M. Cuevas and H. Fritzsche (unpublished).

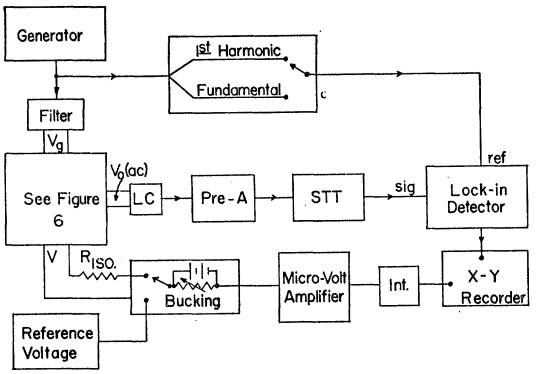

FIG. 7. Block diagram of electronic circuit used to measure dI/dV [$I(f)$] and d^2I/dV^2 [$I(2f)$]. STT is a narrow-band amplifier and Int. is a passive integration network.

was filtered to reject the fundamental by resonating the transformer's self-inductance L_H at the first-harmonic frequency with a capacitor (LC block—Fig. 7) to cut down the distortion in the preamplifier (Pre A block—Fig. 7).

The output of the preamplifier (Fig. 7) was fed into a narrow-band amplifier (STT block—Fig. 7) to reduce the noise component away from the signal frequency as well as to further reduce the fundamental when measuring $I(2f)$. Finally the output of the narrow-band amplifier was detected by a lock-in amplifier whose reference signal came from a harmonic generator driven by the audio generator (Fig. 7). The dc output was integrated from 0.1 to 3.0 sec and recorded on the Y axis of the X-Y recorder. The conductance range available in the current amplification circuit was 1.2×10^{-6} mho to 1.1×10^{-10} mho with a distortion of less than $10^{-2}\%$. The noise level was around 8×10^{-11} A for a 3-sec integration time. A frequency of 100 cps was used for the fundamental when measuring $I(f)$ and 50 cps when measuring $I(2f)$. Results were checked for capacitive effects at 40 and 20 cps with no observable differences.

Accurate measurement of the dc voltage V across the tunnel junction (Figs. 6 and 7) was important for measuring accurately the threshold voltages V_t. Part of the voltage drop V was canceled by a bucking potential (bucking block—Fig. 7) to increase the sensitivity of the voltage measurement around a given bias. V was calibrated absolutely by substituting a reference potential (reference voltage block—Fig. 7) before the bucking potential. While it was not necessary to use amplification to record continuously the dc voltage, a dc amplifier (microvolt amplifier block—Fig. 7) was used to minimize the current drawn through the voltage leads. An input impedance in excess of 90 MΩ was used. No indication of current-induced voltage drops was found in the experiment.

After amplification, the dc voltage was integrated (Int. block—Fig. 7) and recorded on the X axis (X-Y recorder block—Fig. 7). The integration reduced the ac signal noise and compensated for the integration time in the Y axis. Noise was further reduced by "guarding" the voltage leads with an inner shield from the cryostat to the dc amplifier. The dc recorded voltage was isolated from the ac voltage drop across the junction by a 1-MΩ isolating resistance R_{Iso} (Fig. 7) and the integration circuit. The over-all noise level of the circuit was 1 μV with a long-term stability of 5 μV/day. The thermoelectric voltage was frequently measured and did not vary by more than 1 μV during any measurement.

C. Determination of the Current Derivatives

The derivatives dI/dV and d^2I/dV^2 are related to $I(f)$, $I(2f)$, and V_{ac} by assuming the tunnel junction to be a current source[27] I(dc, ac) (Fig. 6) and expanding in powers of the applied voltage drop ΔV under the condition $\Delta V \ll V_0$. For this experiment $\Delta V = V_{ac} - I_{ac}R$, where R is the series resistance of all elements in the low-impedance circuit except the sample, i.e., lead resistance, transformer impedances, etc. (see Fig. 6).

By reiteration, we find

$$I(f)=\frac{dI}{dV}\left(1+\frac{dI}{dV}R\right)^{-1}V_{ac}+\text{const}\frac{d^3I}{dV^3}V_{ac}^3, \tag{3}$$

$$I(2f)=(2)^{-3/2}\frac{d^2I}{dV^2}\left(1+\frac{dI}{dV}R\right)^{-3}V_{ac}^2+\text{const}\frac{d^4I}{dV^4}V_{ac}^4, \tag{4}$$

where $I(f)$, $I(2f)$, and V_{ac} are now the measured rms values.

Equations (3) and (4) were checked experimentally to within 5% for the circuit resistance of $R=30\pm1.5\ \Omega$.

The above equations yield dI/dV and d^2I/dV^2 only in the limit as $V_{ac}\to 0$. Experimentally, at 4.22°K V_{ac} had to be less than 100 μV, and at 1.15°K V_{ac} had to be less than 50 μV in order to determine dI/dV and d^2I/dV^2 to within 1% for the rapidly varying line shapes observed in this experiment.

In this experiment, the major results center around the analysis of the (d^2I/dV^2-V) curve near the threshold voltage $V=V_t$. It is therefore important to show examples of the determination of (d^2I/dV^2) from $I(2f)$ in the voltage region, the peak voltage, and the half-width.

The solid line in Fig. 8 shows the recorder trace for the LA forward bias peak of junction $D1B$ at 1.15°K. The horizontal scale has been expanded by inserting in the circuit a constant bucking voltage. The voltage recorded on the vertical axis is related to d^2I/dV^2 through Eq. (4). The sampling voltage V_{ac} was sufficiently small to keep the contributions of the higher order terms in Eq. (4) below 1%. The bias was swept at a rate of 0.3 mV/min to achieve an integration time of 3 sec.

[27] G. R. Branner, E. M. Friar, and G. Medicus, Rev. Sci. Instr. 34, 231 (1963).

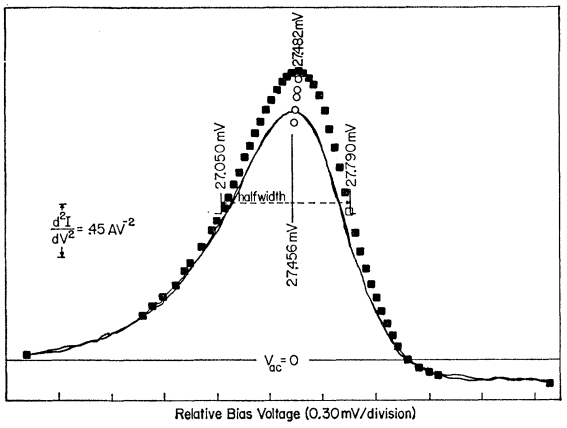

FIG. 8. Example of corrections made to experimental $I(2f)$ versus V plots in order to obtain (d^2I/dV^2-V) line shapes. Original curves of $I(2f)$ for the positive bias LA peak at 1.15°K (solid lines) are corrected by Eq. (4) to obtain d^2I/dV^2 (squares). Vertical mark (27.456 mV) is the calibration mark for scale. The sensitivity is 0.300 mV/division. The d^2I/dV^2 peak voltage (27.482 mV) was found by the behavior of circles. Half-width is also indicated. The resulting curve in normalized units is plotted (filled squares) in Fig. 10(b).

In order to obtain d^2I/dV^2 from this curve one has to correct for the factor $[1+(dI/dV)R]^{-3}$ in the first term in Eq. (4). R and dI/dV were measured to within 10% absolute and 1% relative error in order to obtain the d^2I/dV^2 curve shown by the squares in Fig. 8. The relative magnitudes of the d^2I/dV^2 values are correct to within 2% and the absolute magnitude scale of Fig. 8 has an accuracy of about 10%. The line marked $V_{ac}=0$ defines the zero of the vertical scale. The vertical lines in Fig. 8 mark the voltage calibration of the bias scale.

Figure 8 also shows the technique for finding the peak voltage and half-width. The voltages of the intercepts of the curve with a given ordinate value were averaged as shown by the circles. A plot of these points asymptotically approaches the best value for the peak voltage as the ordinate value approaches the peak amplitude. An average, called the peak voltage V_p, of the absolute magnitude of forward and reverse bias-peak voltages was taken to cancel out the thermoelectric voltages. It must be noted that although Eq. (5) introduces higher even-order derivatives when V_{ac} is large, all the derivatives have the same symmetry relative to V_p. Experimentally, the averaged value V_p of the different phonon branches was independent of V_{ac} from 0 to 300 μV rms. The half-peak amplitude voltages are also indicated. The difference between these voltages determines the halfwidth of the peak.

IV. ANALYSIS OF EXPERIMENTAL RESULTS

For all the junctions of antimony-doped base material used in this experiment, the I-V curves have the same qualitative characteristics, once the differences in I_p and I_V are taken into account. This is also true for the (dI/dV-V) and (d^2I/dV^2-V) curves. Table III lists the average peak voltages V_p and average halfwidths H obtained from (d^2I/dV^2-V) curves for tunnel junctions with major tunnel currents along the (110) and (100) directions taken at 1.15°K. In several cases (footnote to Table III), the ac voltage V_{ac} was too large and it was necessary to find a value for the average half-width by extrapolation. For the type of distortion present, it is reasonable to assume that the half-width has the form $H(V_{ac})=H+Z(V_{ac})^2$ for a given temperature. Experimentally, plots of $H(V_{ac})$ fit the equation to within 5%. For each peak, the constant Z was determined and H was obtained from the available data. Finally, rough determinations of the peak voltages to within ± 0.2 mV and average halfwidths to within 10% for tunnel currents along the (111) direction (junctions $B1A$ and $B1B$) agree well with the results from the other tunneling directions.

The major conclusion drawn from these results is that the major factors that contribute to the d^2I/dV^2 peak voltage and line shape are independent of crystallographic direction to within ± 0.2 mV and 10%, respectively. Another conclusion that can be reached is that for a given tunneling direction internal strains, variations in n-type concentration, peak current and valley current did not play a large role in the measurement of the peak voltage and half-width. Therefore, only one junction, $D1B$, will be used for a detailed analysis. This sample has also been used for illustrative purposes in the earlier sections, Figs. 1–3, 8.

In the following sections, figures of the individual peaks are normalized by assigning to the d^2I/dV^2 peak amplitude the value one and the prethreshold amplitude the value zero. The bias (abscissa) is plotted in units of $e(V-V_p)/kT$, where V and V_p are the absolute

TABLE III. d^2I/dV^2 peak voltages and average half-widths at 1.15°K.

Junction name	Peak voltage TA (±0.005 mV)	LA (±0.008 mV)	LO (±0.02 mV)	TO (±0.02 mV)
A1A	7.806	27.490	30.54	36.05
A1B	7.807	27.494	30.53	36.04
A2A	7.808	27.493	30.56	36.05
A2B	7.803	27.483	30.56	···
A3A	7.807	···	30.55	36.05
A3B	7.803	···	···	···
D1A	7.806	···	30.57	36.03
D1B	7.810	27.496	30.55	36.03
Junction name	**Half-width TA (±0.01 mV)**	**LA (±0.01 mV)**	**LO (±0.04 mV)**	**TO (±0.04 mV)**
A1A	0.56	0.73	0.84	0.73
A1B	···	···	···	···
A2A	0.56[a]	0.76[a]	0.85[a]	0.71[a]
A2B	0.57[a]	0.77[a]	0.83[a]	···
A3A	0.57[a]	···	0.81[a]	0.71[a]
A3B	0.56[a]	···	···	···
D1A	0.57[a]	···	0.88[a]	0.70[a]
D1B	0.57	0.74	0.88	0.68

[a] Data obtained by extrapolation of the form $H(V_{ac})=H+Z(V_{ac})^2$ where the constant Z is determined by other samples for the same branch.

magnitude of the bias voltage and peak voltage. For comparison purposes at a given temperature, the negative bias peak (open points) and the positive bias peak (full points) are in the same figure. A simple line shape is also plotted (dashed line) in each figure. The relative error in the ordinate of the normalized peaks is indicated by an error bar or by the size of the symbols for the individual points. The abscissa has an error of less than 1% of the full scale value.

In order to have an absolute comparison for the peak amplitudes at 4.22 and 1.15°K Table IV is provided.

A. Step-Function Distortion

It can be qualitatively seen from Fig. 3 that all the distinguishable d^2I/dV^2 peaks have step-function distortions similar to that shown in Fig. 4(b). It appears that this distortion has a similarity to the dI/dV-V curve (Fig. 2). This view is strengthened by the experimental observation that, as T is changed from 4.2 to 1.15°K, the amplitudes of the distortion and dI/dV are independent of temperature at bias voltages outside the kT broadened threshold region.

The relation between the step-function distortion and dI/dV can be seen from the derivative of Eq. (1) with respect to voltage. If G is considered constant in E, then

$$\frac{dI}{dV}=\sum_{E_{b(q)}}\left\{-G\int f\frac{df(V)}{dV}dE \qquad (5a)\right.$$

$$\left.+\frac{dG}{dV}\int f[1-f(V)]dE\right\}. \qquad (5b)$$

Again, terms like (5b) can be ignored for they are roughly constant in the region of interest. Terms (2b) and (5a) differ only by the ratio $2(dG/dV)G^{-1}$. Because of the consistent similarity of the step-function distortion with dI/dV, it is clear that the ratio $2(dG/dV)G^{-1}$ changes only slightly with V from positive to negative bias peak voltage. As previously mentioned, it follows that the average peak voltage V_p can be considered roughly independent of the effect of this distortion. For the same reason the average of the line shapes for positive and negative bias shown in the Figs. 9, 10, 13, and 14, can be considered roughly independent of the step-function distortion.

TABLE IV. d^2I/dV^2 peak amplitudes for junction $D1B$.

Branch[a]	Peak amplitude 4.2°K Relative to zero AV^{-2}	4.2°K Relative to prethreshold AV^{-2}	1.15°K Relative to zero AV^{-2}	1.15°K Relative to prethreshold AV^{-2}
TO+	0.113	0.266	0.668	0.774
LO+	...	...	0.734	0.867
LA+	0.876	0.918	2.48	2.48
TA+	0.595	0.595	2.17	2.17
TA−	−0.590	−0.590	−1.88	−1.88
LA−	−1.17	−1.10	−3.04	−2.87
LO−	...	...	−0.875	−0.656
TO−	−0.405	−0.137	−0.713	−0.397

[a] Positive bias denoted by + and negative bias denoted by −.

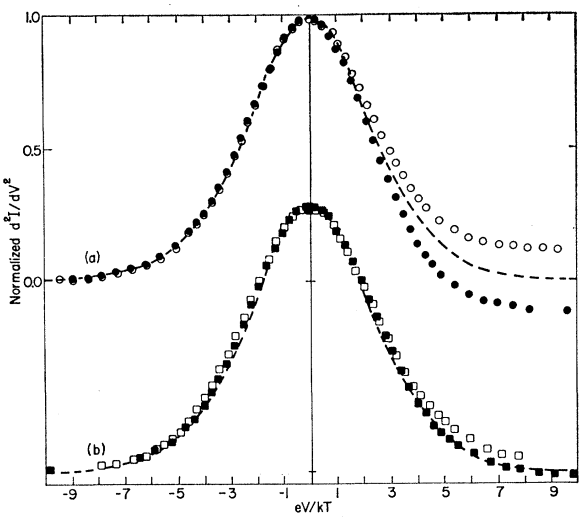

FIG. 9. The TA branch line shapes in normalized units at two temperatures. The peak amplitudes are normalized to unity relative to the prethreshold amplitudes. The absolute magnitude of the bias voltage minus the absolute magnitude of the peak voltage is plotted in dimensionless units eV/kT. Filled symbols refer to the positive bias peak. Open symbols refer to the negative bias peak. Circles symbolize data at 4.2°K (a). Squares refer to 1.15°K data (b). A simple line shape is plotted in a dashed line.

For quantitative results at 4.2°K, the TA branch line shapes [Fig. 9(a)], when averaged, agree with the simple line shape to within the experimental error. The average half-width H of this peak at 4.2°K is 1.96±0.03 mV. This agrees with the simple line shape value of 1.969 mV. The good agreement of these quantitative results indicate that, at least for the TA branch, the function G has a variation with respect to V and E of less than the experimental error (2%) over the bias region of the line shape as well as being only slightly dependent upon V over the bias range from positive to negative bias-peak voltage.[28] Therefore, the average line shape and V_p are independent of the distortion for the TA branch.

The presence of the dispersion broadening distortion and considerable overlap between peaks at 4.2°K, make it difficult to analyze quantitatively the LA, LO, and TO branches in the same way as the TA. However, because dI/dV and the step-function distortion are independent of temperature below 4.2°K (once the Fermi functions are accounted for) and the term (2a)

[28] This result was checked with the Keldysch-Kane theory (Refs. 1 and 2). For the TA branch, the ratio $2(dG/dV)G^{-1}$ was calculated to be 20.4 V^{-1} for both positive and negative bias peaks by using Kane's Eq. (33), the relevant quantities for junction $D1B$, and assuming an abrupt junction. The ratio was found to be 60±5 V^{-1} for both peaks in the experiment. Agreement to better than an order of magnitude is not expected because the theory does not adequately explain the voltage dependence of the tunneling current.

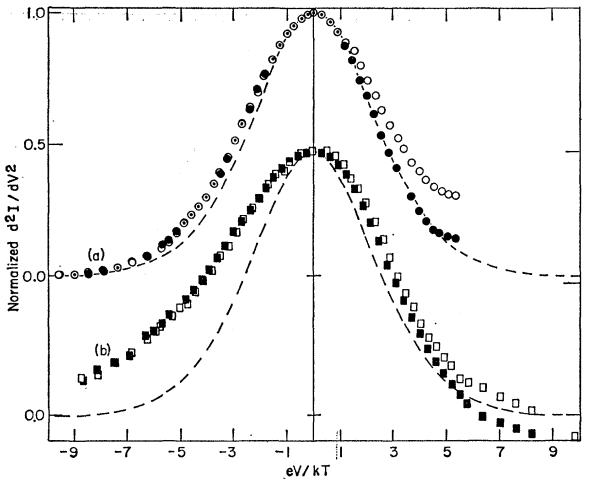

FIG. 10. The LA branch line shapes in normalized units at two temperatures. The peak amplitudes are normalized to unity relative to the prethreshold amplitudes. The absolute magnitude of the bias voltage minus the absolute magnitude of the peak voltage is plotted in dimensionless units eV/kT. Circles (a) refer to 4.2°K results for positive (filled) and negative (opened) bias. Filled squares refer to positive bias peak at 1.15°K. Open squares to the negative bias peak at 1.21°K. The simple line shape is plotted in the dashed line.

rapidly increases as T decreases, the effect of the step-function distortion on the line shape rapidly becomes negligible as T is decreased. This can be observed in Figs. 9, 10, 13, and 14. At lower temperatures (part b of figures) the differences in line shape between positive (full points) and negative (open points) bias is much smaller than at 4.2°K (part a). Therefore, even though the step-function distortion of the LA, LO, and TO branches may have a slightly greater voltage dependence for G than the TA branch its effect on the average line shape and V_p is negligible around 1.15°K.

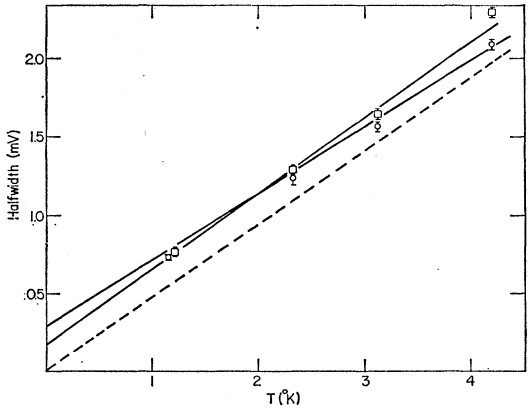

FIG. 11. The LA line shape versus temperature. Both the positive (circles) and negative (squares) bias half-widths are plotted. The extremal slopes indicated by the solid straight lines have positive intercepts at $T=0$. Simple line shape half-width is plotted in the dashed line.

B. Phonon Broadening

In Fig. 9(b), the TA branch at 1.15°K deviates a small but significant amount from the simple line shape (dashed line). This deviation is even more striking for the LA branch at both 4.2 and 1.15°K [Fig. 10(a) and (b)]. The half-widths of the positive and negative bias peaks are plotted as a function of temperature in Fig. 11, revealing the fact that all the slopes through all the points have a positive intercept at $T=0$°K. A plot of the LA average peak voltage versus T (Fig. 12) reveals a considerable increase in peak voltage as $T\rightarrow 0$. A similar plot of peak voltage for the LO peak indicated a decrease as $T\rightarrow 0$. Further, an asymmetry factor S may be defined as $S=(|V_u-V_p|-|V_l-V_p|)/H$, where V_u is the half-peak voltage that is larger than V_p in absolute magnitude and V_l is the half-peak voltage that is smaller in absolute magnitude. At 1.15°K one can immediately see that for the LA branch [Fig. 10(b)], S is less than zero while for the LO branch

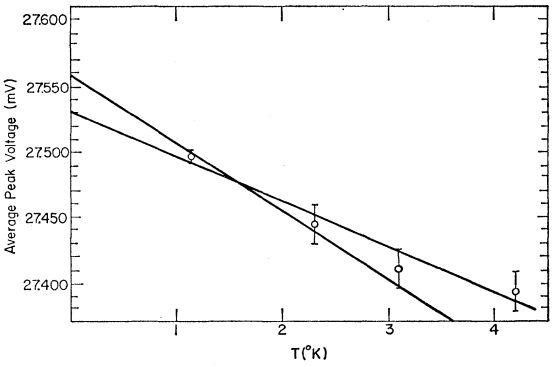

FIG. 12. The average peak voltage of the LA branch versus temperature. The extremal slopes indicated by the solid straight lines show V_p increases between 4.2° and 1.15°K.

(Fig. 13), S is greater than zero. The TO branch [Fig. 14(b)] reveals little apparent asymmetry but still has a large broadening. All of these effects can be interpreted in terms of the phonon-dispersion distortion.

Quite a wide difference in phonon dispersion can be seen in the phonon spectrum as determined by neutron spectroscopy (Fig. 15). The phonon spectrum from $\Gamma\rightarrow L$ is obtained from the work of Brockhouse and Iyengar[5] (crosses in Fig. 15). The sign of the curvatures of each branch from $L\rightarrow K$ (solid lines), the (110) intersection with the BZ boundary, can be estimated from the phonon energies at the point X, the (100) intersection with the BZ boundary. This spectrum shows that the energy surfaces of the different phonon branches are hyperbolic near the point L.

A coordinate system can be defined as $\hat{q}_l$, the unit vector along the line $L\rightarrow\Gamma$, and $\hat{q}_t$, the unit vector along $L\rightarrow K$. Only two coordinates are needed because of the threefold rotation symmetry about $\hat{q}_l$ at L. Two cases

are possible for the hyperbolic energy surfaces:

case A, $E_b=E_b(\mathbf{q})-E_b(L)=(\frac{1}{2})\alpha(q_t)^2-(\frac{1}{2})\beta(q_l)^2$

the energy surface of the TA and LA branches; and

case B, $E_{b'}=E_{b'}(\mathbf{q})-E_{b'}(L)=(\frac{1}{2})\beta(q_l)^2-(\frac{1}{2})\alpha(q_t)^2$

the energy surface of the LO and TO branches. Only case A will be considered, for it can be transformed into case B by substituting $E_b \Rightarrow -E_{b'}$.

The energy surfaces are not closed near L and some external cutoff must be imposed to limit the sum over $E_b(\mathbf{q})$ of Eq. (2) to find the effect of the phonon dispersion. As previously mentioned, a rough choice for the cutoff is the Fermi surfaces. The sum of the two Fermi surfaces can be approximated by an ellipsoid of revolution about $\hat{q}_l$ centered at L with a semimajor axis of K_l along $\hat{q}_l$ and semiminor axis of K_t along q_t. By ignoring the $\mathbf{q}$ and $E_b(\mathbf{q})$ dependence of G, the sum

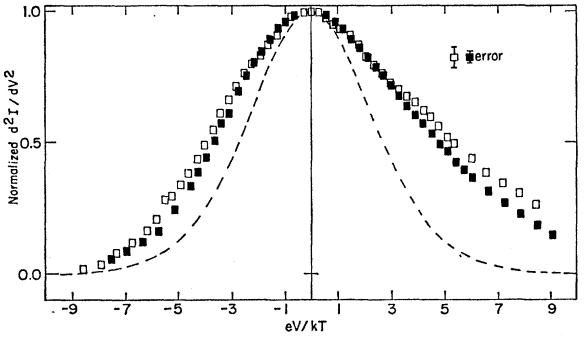

FIG. 13. The LO-branch line shapes in normalized units. The peak amplitudes are normalized to unity relative to the prethreshold amplitudes. The absolute magnitude of the bias voltage minus the absolute magnitude of the peak voltage is plotted in dimensionless units eV/kT. Filled squares refer to positive bias at 1.15°K. Open squares refer to negative bias at 1.21°K. The simple line shape is plotted in the dashed line.

over $E_b(\mathbf{q})$ can be converted into an "effective" phonon density of states integral. The resulting "effective" density of states is

$$\frac{dn}{dE}=\frac{A^{-3/2}}{\kappa}\left(\frac{\alpha K_t^2}{2}-E_b\right)^{1/2}, \qquad E_b\geq 0$$

$$\frac{dn}{dE}=\frac{A^{-3/2}}{\kappa}\left[\left(\frac{\alpha K_t^2}{2}-E_b\right)^{1/2}-\left(\frac{\alpha}{\beta}\right)^{1/2}\kappa(-E_b)^{1/2}\right], \qquad E_b\leq 0 \quad (6)$$

where $\kappa=[(\beta/\alpha)+(K_t^2/K_l^2)]^{1/2}$ and A is a numerical factor which is the same for all the peaks. For the limiting case $E_b \ll \alpha(K_t)^2/2$, the result fits the general density of states for saddle points given by Ziman.[29]

It can be seen from the calculation that the density

[29] J. M. Ziman, *Principles of the Theory of Solids* (Cambridge University Press, London, 1964), Chap. 2, p. 49.

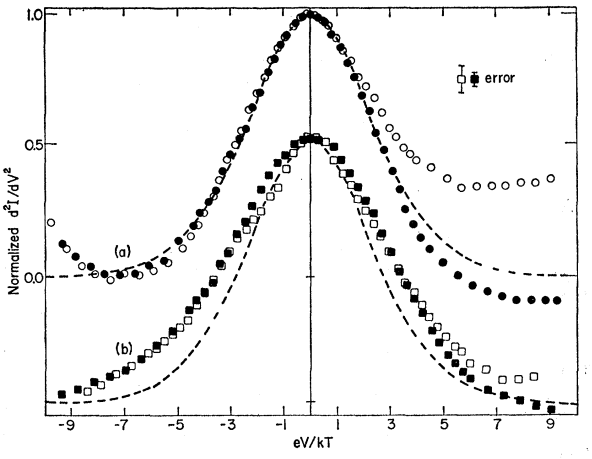

FIG. 14. The TO-branch line shapes in normalized units at two temperatures. The peak amplitudes are normalized to unity relative to the prethreshold amplitudes. The absolute magnitude of the bias voltage minus the absolute magnitude of the peak voltage is plotted in dimensionless units eV/kT. Circles (a) refer to 4.2°K results for positive (filled) and negative (open) bias. Filled squares refer to positive bias at 1.15°K. Open squares refer to the negative bias peak at 1.21°K. The simple line shape is plotted in the dashed line.

of states depends rather sensitively on $\alpha(K_t)^2$ and $\beta(K_l)^2$. If $\beta(K_l)^2$ is much larger than $\alpha(K_t)^2$, then a peak approaching that of Fig. 4(c) is obtained. However, if $\beta(K_l)^2$ is much smaller than $\alpha(K_t)^2$ then the density of states is effectively zero for $E_b<0$, has a positive nonzero value at $E_b=0$, and slopes off slowly to zero for $E_b>0$.

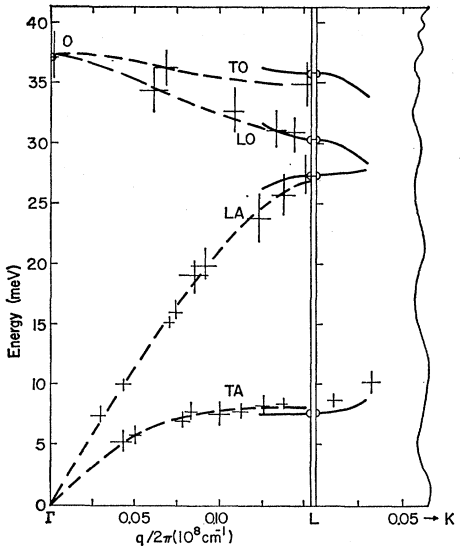

FIG. 15. Part of the phonon spectrum of germanium. The $\Gamma \rightarrow L$ curves (dashed lines) are taken from the work of Brockhouse and Iyengar (crosses, Ref. 5). The sign of the $L \rightarrow K$ curvatures (except the TA branch) are estimated from the phonon energies at X (solid lines). The TA branch $L \rightarrow K$ curvature comes from the work of Brockhouse and Iyengar. Half-circle symbols indicate the phonon energies determined by this paper. Solid lines show curvatures obtained by this work.

TABLE V. Comparison of line shape parameters of junction *D1B* with best-fit values of phonon-density-of-states sum at finite temperature.

Branch	H (4.22°K) mV	$\Delta V_p = V_p(1.15) - V_p(4.2)$ mV	H (1.15°K) mV	S (1.15°K)	α (10^{-15} meV-cm^2)	β (10^{-15} meV-cm^2)	$E_b(L) - V_p$ (1.15°K) mV
Simple line shape	1.969	0.00	0.537	0.0	...	...	0.0
TA							
Exptl.	1.96±0.03	0.0 ±0.015	0.57 ±0.01	0.015±0.015	...	...	...
theory	1.99±0.01	0.0 ±0.005	0.57 ±0.005	0.016±0.005	7.9	1.1	−0.04
NS[a]	...	...	...	...	7.9	0.0	...
LA							
Exptl.	2.20±0.03	0.103±0.01	0.75 ±0.01	−0.15 ±0.01	...	...	...
theory	2.12±0.01	0.093±0.01	0.76 ±0.005	−0.17 ±0.01	4.0	9.0	+0.087
NS[a]	...	...	...	...	...	18.0	...
LO							
Exptl.	...	−0.065±0.02	0.89 ±0.04	0.11 ±0.01	...	...	...
theory	...	−0.105±0.02	0.89 ±0.005	0.12 ±0.01	19.0	9.0	+0.064
NS[a]	...	...	...	...	...	4.45	...
TO							
Exptl.	2.12±0.03	0.0 ±0.02	0.68 ±0.04	0.0 ±0.01	...	...	...
theory	2.02±0.01	0.0 ±0.02	0.66 ±0.005	0.0 ±0.01	16.0	2.2	+0.110
NS[a]	...	...	...	...	...	1.12	...

[a] Estimates of curvatures taken from neutron spectroscopy data. See Ref. 5.

In order to get adequate quantitative results for comparison with the experimental values of S, H, and the change in peak voltage ΔV_p with T, it is necessary to integrate over the product of the simple line shape and the "effective" density of states. A computer was employed to find the best fit for α and β for a given K_l and K_t at two temperatures, 4.22 and 1.15°K.

The values for K_l and K_t were found by summing the extremal dimensions of the conduction- and valence-band Fermi surfaces parallel and perpendicular to $\hat{q}_l$, respectively. It has been shown that the light-hole band dominates over the heavy-hole band for the valence-band part of the tunneling process.[2] Therefore, by approximating the light-hole surface by a sphere, the extremal dimension is $K^2 = 2m^* E_f \hbar^{-2}$ where $m^* = 0.04\ m_0$, $E_f = 140$ meV, and $\hbar$ is Planck's constant in the appropriate units. Similarly, the ellipsoidal conduction-band extremal values are found where $m_l = 1.64\ m_0$ and $m_t = 0.082\ m_0$ for extrema parallel and perpendicular to

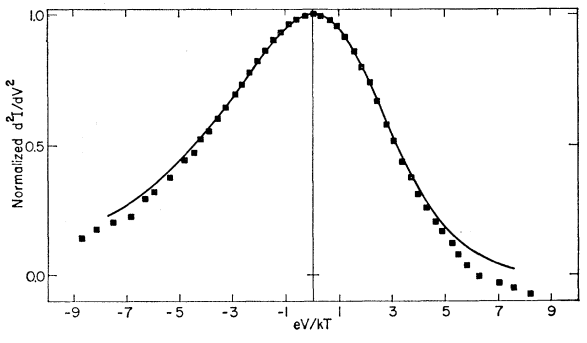

FIG. 16. Comparison of LA line shape with phonon "effective" density of states calculation for 1.15°K. The positive bias LA line shape [filled squares in Fig. 10(b)] is compared with the calculation. The curvatures used are given in Table V.

q_l, and $E_f = 36$ meV for the junction *D1B*. Summing over the extremal dimensions the values $K_l = 17.2 \times 10^6$ cm^{-1} and $K_t = 7.0 \times 10^6$ cm^{-1} are found. These values correspond to roughly 18% and 7%, respectively, of the $\Gamma \rightarrow L$ distance. The comparison of theory with the experiment for the $\Delta V_p = V_p(1.15°\text{K}) - V_p(4.22°\text{K})$, H, and S is given in Table V along with the best-fit curvatures α and β. Because of the overlap of the LA, LO, and TO peaks at 4.22°K, it was anticipated that the LA and TO experimental half-widths would be larger than theory and that the experimental change in peak voltage of the LO would be smaller than theory as indicated in the table.

To show the over-all fit of the line shape, Fig. 16 gives the experimental points (squares) and the calculated curve (solid line) for the LA peak. It is felt that the agreement is sufficiently good to explain the broadening effects observed in the experiment. The uncertainties of the model are then reduced to the uncertainties in finding the curvatures α and β.

The agreement of the curvatures with estimates from the work of Brockhouse and Iyengar (Table V and solid curves in Fig. 15) is within a factor of 2. No better comparison can be made because of the uncertainties in the neutron spectroscopy data, the inaccuracies in obtaining K_t and K_l, the possibility of having G dependent upon $\mathbf{q}$ and $E_b(\mathbf{q})$, and the presence of phonon lifetime broadening.

The Keldysch-Kane theory[1,2] clearly indicates that while momentum transverse to the principal tunneling direction is conserved, the momentum parallel to the tunneling direction is not. It can be shown that the only factor that limits the sum over $E_b(\mathbf{q})$ in the principal tunneling direction is the tunneling matrix element of G. For the junction *D1B* the tunneling direction is effectively along q_t. This means K_l is conserved while one

direction of K_t is not. Because of the sensitivity on αK_t^2 and βK_t^2 this effect could immediately be seen in the comparison of neutron spectroscopy data with this experiment if $G(\mathbf{q})$ is effectively cut off by more than a factor of $\sqrt{2}$ of K_t. In the Keldysch-Kane theory the effective cutoff (half value point) is also roughly 7% of the $\Gamma \rightarrow L$ distance.[30] Other materials will have to be used to resolve these two interpretations.

Phonon lifetime broadening may also be present. This effect due to the uncertainty principle adds a temperature-independent broadening to the simple line shape. The temperature-independent part of the half-width H_0 is the energy uncertainty $H_0 \geq h/\tau$ where τ is the phonon lifetime. The most pessimistic guess for the half-width due to the uncertainty principle is roughly the difference between the TA half-width and the simple-line-shape half-width at 1.15°K, $H_0 < 0.04$ mV. The lifetime τ would then be $\tau \geq 1.6 \times 10^{-11}$ sec. Thermal conductivity data indicate the lifetimes are considerably longer than this value.[31] If this broadening was present it might effectively reduce the values for α without changing β in the LO and TO branches.

In Sec. A, it was shown that the step-function distortion could effectively be canceled by averaging the peak voltage for each branch. Furthermore, as the temperature is lowered the error introduced by this distortion becomes negligible. The experiment shows that the 1.15°K values of the peak voltage listed in Table III are independent of the errors made by the step-function distortion to within the experimental errors listed.

In this section it was shown that phonon broadening effects due to an "effective" phonon density of states dominates at low temperatures and that by computation good agreement for the line shapes could be found. In column 8 of Table V, the discrepancy $E_b - V_p$ between the phonon energy and the 1.15°K peak voltage has been determined for the best fit of α and β. Using the values from Table III, the phonon energies are determined: $E_{TA}(L) = 7.766 \pm 0.007$ meV; $E_{LA}(L) = 27.58 \pm 0.01$ meV; $E_{LO}(L) = 30.62 \pm 0.02$ meV; and $E_{TO}(L) = 36.14 \pm 0.02$ meV. These results are also listed in Table I and in Fig. 15 for comparison with previous experiments.

While there may be still some argument about the precise value of $E_b - V_p$ through inaccuracies mentioned in determining α and β, the author feels confident that other effects do not play a role in determining $E_b(L)$. Therefore, if the need exists, the accuracy can be increased as $T \rightarrow 0$.

C. Double-Phonon Emission

During the course of this experiment, a search in the bias region ± 100 meV was also made for peaks in the $(d^2I/dV^2\text{-}V)$ curve other than those treated in detail in the previous sections. Aside from zero bias effects,[32] only the four peaks shown in Fig. 17 were observed for the impurity concentration range of this experiment. The d^2I/dV^2 scale has been greatly expanded and the zero line shifted off the upper edge of Fig. 17. These peaks appear at bias voltages which roughly correspond to double-phonon emission involving the optic branch at Γ, denoted by $O(\Gamma)$. They are the $TA(L)+O(\Gamma)$, $LA(L)+O(\Gamma)$, $LO(L)+O(\Gamma)$, and $TO(L)+O(\Gamma)$. With these assignments, the energy of $O(\Gamma)$ is given as $E_O(\Gamma) = 37.3 \pm 0.2$ meV (see Fig. 15).

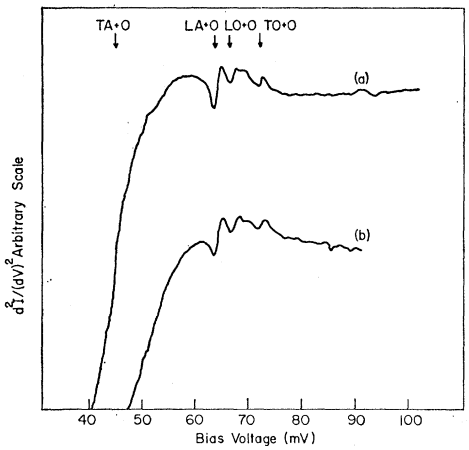

FIG. 17. Double-phonon emissions. Peaks in the $(d^2I/dV^2\text{-}V)$ characteristic at 1.15°K indicate the presence of double-phonon emission processes involving the optic branch O at Γ. The results from two junctions are plotted, curve *a*, *A1A*; and curve *b*, *D1B*. Scale is greatly expanded with zero shifted off the upper edge of drawing.

In the analysis of the double-phonon emission peaks, the best fit for the energy value of $O(\Gamma)$ for the four peaks is not at peak amplitudes but at the more positive point of maximum slope. Several things may explain this. First, the background may distort the peaks enough to cause changes in peak voltages. Second, the point $O(\Gamma)$ is an extremum in the dispersion curves of the TO and LO branches (see Fig. 15). Therefore, the density of states near $O(\Gamma)$ follows the parabolic square root law $(E - E_O(\Gamma))^{1/2}$ and is zero at $O(\Gamma)$. Third, it has been hypothesized that because the transition involving $O(\Gamma)$ is at the zone center, it is affected the same way as the zero bias region is affected. Further experimental and theoretical work will be needed to resolve this interpretations.

D. Verification of the Stress Dependence

In Sec. B, the effect of phonon dispersion on the phonon energy $E_b(L)$ was determined. It is certain that the peak voltage is not exactly the phonon energy at the symmetry point L due to the phonon "effective"

[30] H. Fritzsche (private communication).
[31] M. G. Holland, Phys. Rev. **132**, 2461 (1963).
[32] R. A. Logan and J. M. Rowell, Phys. Rev. Letters **13**, 404 (1964).

density of states. However, it is also certain that the "effective" phonon density of states will not cause a change in peak voltage under stress unless the half-width changes considerably under stress. Experimentally, the half-width did not change to maximum stress of 9×10^9 dyn/cm^{-2} for all cases of stress along the [001] direction (see Table II). For stress along the [011], the analysis is not as clear. There is half-width broadening due to nonequivalence of all the L symmetry points. These results show that at least the pressure or dilation dependence of the peak voltages, previously reported,[8] is that of the phonon energies. Finally, an attempt to measure $O(\Gamma)$ with stress through the double-phonon transitions proved inconclusive. A different type of dopant may be needed to get this information.

V. SUMMARY

The phonon energies at the point L in the Brillouin zone of germanium were found to an accuracy of 0.1% (bottom of Table I). The curvatures of the phonon spectrum at the point L were found to within a factor of 2 (Table V). These energies and curvatures compare favorably with neutron-spectroscopy data (Fig. 15). The high degree of accuracy of the results serves to verify the assumptions made in determining the pressure or dilation dependence of the phonon energies previously reported.[8] Finally, the phonon energy for the optic branch at Γ was obtained as 37.3 ± 0.2 meV.

In order to obtain the above results it was necessary to analyze the line shapes of peaks found in the (d^2I/dV^2-V) curves of antimony-doped germanium p-n junctions. They were adequately analyzed in terms of a major kT broadening effect (simple line shape) and distortions due to a small voltage dependence of the tunneling current $G\,dE$ (step-function distortion) and the phonon dispersion around the point L (phonon-dispersion distortion).

In analyzing the step-function distortion it was found that $G\,dE$ is a smooth, slowly varying function of voltage in the bias region from $+36$ mV to -36 mV. Very little or no voltage dependence of $G\,dE$ was found in the bias region of the individual peaks.

The distortion due to phonon dispersion caused the average peak voltages to vary considerably with temperature. In calculating the phonon-dispersion distortion it was found necessary to impose cutoffs to the sum over phonon wave number. If momentum conservation was assumed in the tunneling process, the cutoffs could be obtained and resulted in an adequate expression for the phonon-dispersion distortion in the form of an "effective" density of states. Theory[1,2] indicates momentum is not conserved along the tunneling direction. Instead it predicts that the tunneling matrix element found in $G\,dE$ rapidly drops to zero at roughly the same value as that indicated by momentum conservation. The experimental results could not resolve the difference between the theory and the momentum-conservation assumption because of the inaccuracies in comparing the curvatures obtained in this experiment with those obtained by neutron spectroscopy.

An estimate of 1.6×10^{-11} sec for the lower limit to the phonon lifetimes at L was made by using the uncertainty principle.

Douple-phonon emission peaks analyzed to obtain the optic-branch phonon energy are not yet fully understood.

ACKNOWLEDGMENTS

The author is indebted to Dr. H. Fritzsche, who has constantly advised and encouraged the author, and to Dr. J. J. Tiemann of the General Electric Company Research Laboratories for valuable advice concerning the preparation of the tunnel junctions. He would like to thank R. N. Hall of the General Electric Company Research Laboratories and Miss L. Roth of Purdue University for the supply of some samples used in this work. It is also a pleasure to acknowledge the technical aid of the Low Temperature Laboratory of The University of Chicago under the general support of the National Science Foundation and the U. S. Atomic Energy Commission.